Bioorganic & Medicinal Chemistry Letters 22 (2012) 738–742

Contents lists available at SciVerse ScienceDirect

Bioorganic & Medicinal Chemistry Letters

journal homepage: www.elsevier.com/locate/bmcl

# Indole RSK inhibitors. Part 2: Optimization of cell potency and kinase selectivity

Thomas M. Kirrane [a,b,*], Stephen J. Boyer [a,†], Jennifer Burke [a], Xin Guo [a], Roger J. Snow [a], Lida Soleymanzadeh [a], Alan Swinamer [a], Yunlong Zhang [a], Jeffery B. Madwed [b,‡], Mohammed Kashem [a], Stanley Kugler [a], Margaret M. O'Neill [b]

[a] Department of Medicinal Chemistry, Boehringer-Ingelheim Pharmaceuticals, Inc., 900 Ridgebury Road, PO Box 368, Ridgefield, CT 06877, USA
[b] Department of CardioMetabolic Diseases Research, Boehringer-Ingelheim Pharmaceuticals, Inc., 900 Ridgebury Road, PO Box 368, Ridgefield, CT 06877, USA

ARTICLE INFO

*Article history:*
Available online 18 October 2011

*Keywords:*
RSK
MAPKAP-K1
Kinase inhibitor

ABSTRACT

A series of inhibitors for the 90 kDa ribosomal S6 kinase (RSK) based on an 1-oxo-2,3,4,5-tetrahydro-1*H*-[1,4]diazepino[1,2-*a*]indole-8-carboxamide scaffold were optimized for cellular potency and kinase selectivity. This led to the identification of compound **24**, BIX 02565, an attractive candidate for use in vitro and in vivo to explore the role of RSK as a target for the treatment heart failure.



Activation of the sodium–hydrogen exchanger (NHE) in myocardial tissue is crucial for pH maintenance during the early phase of cellular stress, such as post myocardial infarction. However, over longer periods, NHE activation leads to $Ca^{2+}$ overload, and eventually cardiac hypertrophy.[1,2] It has been demonstrated that NHE inhibitors can block this process and are efficacious in preclinical models of ischemia-reperfusion injury and heart failure.[3] Several NHE inhibitors reached the clinic, but most were plagued with adverse events that limited their usefulness.[1] It has been hypothesized that the side effects associated with NHE inhibitors could be due to inhibition of NHE's role maintaining basal intracellular pH levels. One way to address this would be to target NHE activation instead of NHE directly. Phosphorylation of NHE by the 90 kDa ribosomal S6 kinase (RSK, also known as mitogen-activated protein kinase-activated protein kinase-1 [MAPKAP-K1]) has been shown to activate NHE under stress conditions and could be a potential point for therapeutic intervention.[4]

In a previous paper, we described the identification of a series of indole lactam RSK inhibitors via a high-throughput screen and their optimization into compounds with moderate cellular potency and acceptable kinase selectivity profiles.[5] In this Letter, we will discuss the SAR for three classes of heteroaromatic amides with a focus on further improvement of cellular potency, kinase selectivity, and physicochemical properties.

Since we were interested in a heart failure treatment that could be administered chronically, we were particularly focused on selecting compounds with the best possible safety profile. Thus, a significant part of our effort centered on optimizing for kinase selectivity. Previous internal experience with several kinase targets had shown that utilizing a single representative off-target kinase to assess selectivity often led to surprising selectivity issues with advanced compounds. For this program, we chose instead to monitor selectivity for key compounds against a panel of 20 kinases (Table 1). The panel was determined by profiling several compounds from the early optimization effort at a single concentration against 226 unique kinases offered by Invitrogen.[6] Those with the highest degree of cross-reactivity with our lead series were selected for the routine panel. Interestingly, we found that affinity profile was driven largely by chemotype and not by kinase homology, consistent with other observations reported in the literature.[7]

It was most efficient to track kinase activity across a panel as percent inhibition at a single concentration of 3 μM. Additionally, through correlation with dose–response experiments, we found that inhibition greater than 80% typically returned an $IC_{50}$ under 1 μM, which would highlight a compound with a potential concern. To aid the comparison of compound kinase selectivity profiles, we instituted a selectivity count, defined as the number of kinases with greater than 80% inhibition. Shown in Table 1 are a non-selective HTS hit **1** along with an example of the oxazole **2**, pyrazole **3**, and benzimidazole **4** classes of amides. It is important to note that this type of qualitative assessment has the greatest utility when comparing compounds of similar RSK potency

Compounds in Tables 1–3 were made via amide coupling of indole lactam carboxylic acid with the corresponding heteroaromatic

* Corresponding author.
*E-mail address:* tom.kirrane@boehringer-ingelheim.com (T.M. Kirrane).
† Present address: Global Regulatory Sciences, Bristol-Myers Squibb, 5 Research Parkway, Wallingford, CT 06492, USA.
‡ Present address: Department of Cardiovascular Diseases, Merck & Co. Inc., 126 E. Lincoln Avenue, PO Box 2000, Rahway, NJ 07065, USA.

0960-894X/$ - see front matter © 2011 Elsevier Ltd. All rights reserved.
doi:10.1016/j.bmcl.2011.10.029

**Table 1**
Kinase selectivity for selected compounds

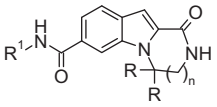

| Compound | 1[a] | 2[a] | 3[a] | 4[a] |
|---|---|---|---|---|
| $R^1$ | 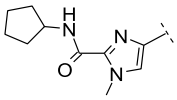 |  | 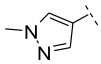 | 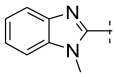 |
| R | Me | H | H | H |
| n | 1 | 2 | 2 | 2 |
| CHEK2 (67) | | | | |
| CLK1 (67) | | | | |
| CLK2 (67) | | | | |
| DYRK1A (63) | | | | |
| FGFR2 (52) | | | | |
| VEGFR2 (63) | | | | |
| LRRK2 (59) | | | | |
| MEK1 (59) | | | | |
| GCK (59) | | | | |
| HGK (52) | | | | |
| PRAK (63) | | | | |
| TRKA (59) | | | | |
| PDGFRa (59) | | | | |
| PRKD1 (67) | | | | |
| RET (52) | | | | |
| AMPK A1/B1/G1 (63) | | | | |
| Aurora A (63) | | | | |
| Aurora B (63) | | | | |
| CDK1/ cyclin B (59) | | | | |
| CDK2/ cyclin A (59) | | | | |
| Selectivity count | 17 | 9 | 9 | 13 |

Homology of ATP pocket as defined by Vieth, et al. versus RSK2 (N-terminal domain) in ().
[a]Green represents <80% inhibition, red is ⩾ 80% inhibition at 3 μM.

**Table 2**
SAR of isoxazolyl and pyrazole amides

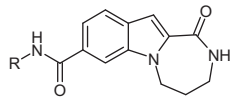

| Compound | R | RSK2 $IC_{50}$[a] (nM) | HLR-CREB $IC_{50}$[11] (nM) | Selectivity count[b] | Aqueous solubility (μg/mL) |
|---|---|---|---|---|---|
| **2** | 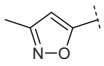 | 19 | 200 | 9 | 8 |
| **8** | 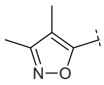 | >10,000 | | | 2 |
| **9** | 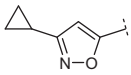 | 18 | 250 | 9 | 21 |
| **10** | 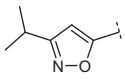 | 26 | 460 | 5 | >35 |
| **11** | 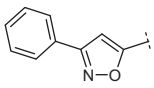 | 86 | 360 | 2 | <0.1 |
| **12** | 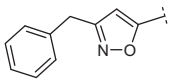 | 13 | 130 | | 0.1 |
| **3** | 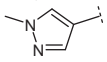 | 11 | 790 | 9 | >32 |
| **13** | 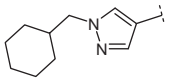 | 7 | 120 | 9 | 0.6 |
| **14** | 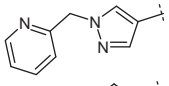 | 10 | 460 | | >40 |
| **15** | 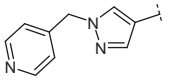 | 2 | 90 | | >40 |

[a] Values are means of at least two experiments, standard deviation is typically 50% reported value.
[b] Selectivity count = number of kinases with >80% inhibition @ 3 μM, 20 total kinases in panel shown in Table 1.

amine left hand side (LHS).[5] 4-Aminopyrazoles were prepared from commercially available 4-nitropyrazole following the literature procedure.[8] The synthesis of 2-aminobenzimidazoles (Scheme 1) began with $S_NAr$ addition of ammonia or a substituted amine to a 2-fluoro-nitrobenzene (**5**) to give aniline **6**. Following reduction of the nitro group, the desired 2-aminobenzimidazole 7 was obtained by condensation with cyanogen bromide. Substituted lactam coupling partners were prepared as previously reported, with the exception that enantiopure (*R*)- and (*S*)-1-Me-lactams were made using enantiopure aminoalcohols.[5]

As previously mentioned, both the isoxazole and pyrazole LHS amides give potent RSK inhibitors with moderate cellular potency and have similar SAR trends.[5] It is worth noting that substitution on these aminoheterocycles adjacent to the amide results in a complete loss of potency, likely as a result of lost planarity between the heteroaromatic ring and the amide (compare **2** and **8**). However, docking studies showed potential for substitution at the 3-postion

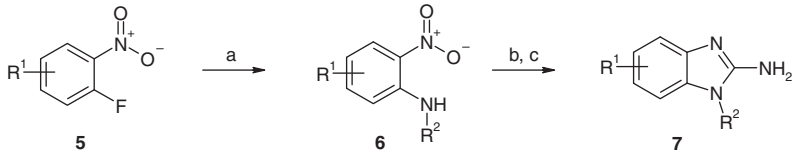


**Scheme 1.** Reagents and conditions: (a) amine, Hunig's base, DMSO, 60 °C, 18 h; (b) ammonium formate, Zn, EtOH, 60 °C, 2 h; (c) cyanogen bromide, EtOH, 18 h, 10–50% (three steps).

**Table 3**
SAR of 2-benzimidazoyl amides

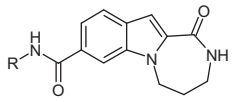

| Compound | R | RSK2 $IC_{50}$[a] (nM) | HLR-CREB $IC_{50}$[10] (nM) | Selectivity count[b] | Aqueous Solubility (μg/mL) |
|---|---|---|---|---|---|
| **4** | 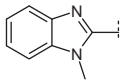 | 9 | 200 | 13 | 21 |
| **16** | 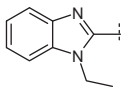 | 1 | 40 | 13 | 3 |
| **17** | 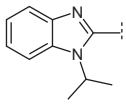 | 20 | 180 | 4 | 12 |
| **18** | 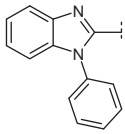 | 61 | 1000 | 9 | 0.1 |
| **19** | 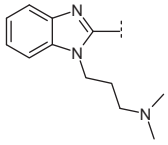 | 21 | 200 | 3 | 39 |
| **20** | 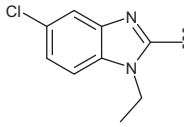 | 6 | 130 | 7 | <0.1 |
| **21** | 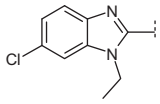 | 12 | 90 | 3 | <0.1 |
| **22** | 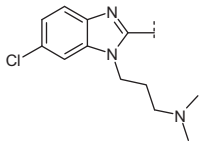 | 20 | 160 | 10 | 29 |
| **23** | 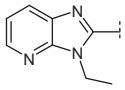 | 4 | 80 | 12 | 2 |

[a] Values are means of at least two experiments, standard deviation is typically 50% reported value.
[b] Selectivity count = # of kinases with >80% inhibition @ 3 μM.

of the ring to reach a pocket that could be filled with larger, lipophilic substituents. The entrance to the lipophilic pocket appears to be narrow, and potency drops off as the steric bulk increased from methyl (**2**) and cyclopropyl (**9**) to isopropyl (**10**) and finally phenyl (**11**). It is also noteworthy that kinase selectivity improves along with steric bulk, as the selectivity count for **2** is 9 while that for **11** is 2. Extending the substituent one carbon further, as in benzyl compound **12**, alleviates any steric clash and results in similar activity to the corresponding methyl analog **2**. The result suggests that the benzyl group is tolerated, but filling the pocket does not provide an improvement in inhibition. An improvement in aqueous solubility is seen as the methyl group is substituted (compare **2**, **9**, and **10**); however, the addition of another aromatic ring in **11** and **12** results in very poorly soluble compounds.[9] In the isoxazole series, we found it difficult to drive down potency while maintaining a reasonable balance of selectivity and solubility.

Similar SAR was observed with pyrazole based amides. Moreover, the chemistry to make the pyrazoles allowed access to a wider range of ring substituents that were not readily achievable in the isoxazole series, such as the cyclohexylmethyl and pyridylmethyl fragments. The similar RSK potency for compounds **13** and **3** demonstrates the size of the lipophilic pocket and also highlights that pi-stacking does not play the same role in the lipophilic pocket as it does with the amide substituent. Introduction of the pyridylmethyl substituents in compounds **14** and **15** gave the expected improvement in aqueous solubility, and also provided the 4-pyridylmethyl compound **15** with a 5-fold boost in potency. While compound **15** fulfilled most of our criteria, it was later discovered to be a potent CYP3A4 inhibitor. Thus we turned to explore other amide substituents.

We also looked at five-membered heterocycles fused to a six-membered ring in the form of benzimidazole analogs such as compound **4** (Table 3). One of the unique characteristics of the benzimidazole amide series is its ability to tolerate substitution adjacent to the amide (compare compound **8** with **4**). This is likely due to the formation of the 2-imino tautomer which simultaneously forces co-planarity as well as provides a hydrogen bond donor interaction with Leu150 (Fig. 1), an effect that has been observed for other amide substitutents in this series.[5] Additionally, the phenyl ring of the benzimidazole forms a key pi stacking interaction with Phe357.

Since benzimadazoyl amides tolerated substitution adjacent to the amide, in contrast to the other series, we set out to explore the SAR at this position. Homologation of compound **4** to give **16** provided a significant boost in molecular and cellular potency, which came at the expense of solubility. Docking suggests the improvement results from the ethyl group fitting into a lipophilic indentation on the floor of the pocket. The additional steric bulk of isopropyl compound **18** shows a similar level of activity to **4** but has significantly improved kinase selectivity. Unfortunately, a further increase in steric demand, as in compound **18**, results in micromolar cellular potency likely due to a clash with the wall of the protein.

Molecular modeling suggested an extension of the ethyl side chain could be tolerated and might allow for interaction with the acidic residues on the floor of the binding pocket. We looked at a number of basic amine containing sidechains of varying lengths where the amine was either acyclic or cyclic, and discovered the dimethylaminopropyl compound **19**. Its RSK potency is maintained at a similar level as methyl compound **4**, while both the aqueous solubility and kinase selectivity were measurably improved.

In addition to investigating substitution on the nitrogen, we also wanted to explore the available space shown by modeling to be adjacent to the phenyl ring of the benzimidazole. Chloro compounds **20** and **21** showed very good potency and good to excellent kinase selectivity, but both were withheld from further profiling due to very poor aqueous solubility. We sought to improve solubility by combining the chloro substituent with the aminopropyl sidechain to give compound **22**. While its solubility is dramatically improved and RSK potency maintained, the selectivity of compound **22** was unexpectedly decreased relative to either **19** or **21**. We also attempted to modulate physicochemical properties by introducing a nitrogen in the fused six membered ring of **16** to give **23**. The compound maintained binding and cellular potency; however, it did not have the intended effect of improving solubility. Of all the benzimidazole analogs we examined, the dimethylaminopropyl substituent consistently offered the best balance of cellular potency, kinase selectivity, and aqueous solubility.

With the aminopropylbenzimidazole LHS in hand, we returned to the lactam ring. It was known from earlier work with a pyridyl

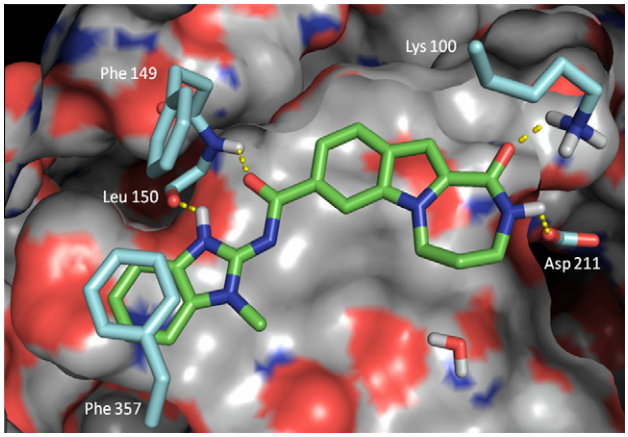


**Figure 1.** Docking of **3** into a crystal structure of RSK2 [30–350] (2.9 Å resolution, Boehringer-Ingelheim unpublished results). The binding mode is based on an X-ray structure for an analogous compound bound to MK2. Dashed yellow lines represent H-bonds <2.5 Å.

**Table 4**
Piperazinone and diazepinone SAR

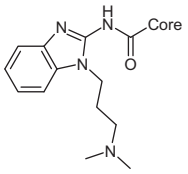


| Compound | Core | RSK2 $IC_{50}$[a] (nM) | HLR-CREB $IC_{50}$[10] (nM) | Selectivity count[b] | Aqueous solubility (μg/mL) |
|---|---|---|---|---|---|
| **24** | 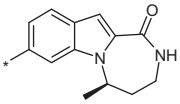 | 1 | 20 | 5 | 26 |
| **25** | 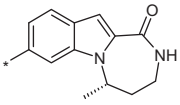 | 14 | 100 | 5 | >45 |
| **26** | 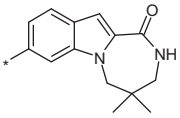 | 27 | 290 | 3 | >50 |

[a] Values are means of at least two experiments, standard deviation is typically 50% reported value.
[b] Selectivity count = # of kinases with >80% inhibition @ 3 μM.

LHS amide that substitution of the lactam ring could enhance potency as well as selectivity. Therefore, we combined the amino-propylbenzimidazole with a number of mono-, di-, and spiro-substituted lactams.[5] In general, the SAR trends for lactam substitution did not differ from what was previously observed for the pyridyl amide series: mono-methylation tended to boost potency while gem-dimethylation, as in **26**, was detrimental (Table 4). We were pleased to see a 14-fold enantiomeric preference for the predicted eutamer (*R*)-**24** over the distamer (*S*)-**25**. This result further supports the docking hypothesis, which suggested one enantiomer of a methyl group adjacent to the indole nitrogen would occupy a small indentation in the roof of the binding pocket. Of the substituted lactam analogs containing the aminopropyl-benzimidazole LHS, compound **24** demonstrated the best combination of potency, selectivity, and solubility and was chosen for further profiling.

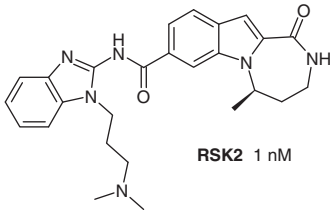


| | | | | |
|---|---|---|---|---|
| **LRRK2** | **PRKD1** | **PRKD2** | **PRKD3** | **RET** |
| 16 nM | 35 nM | 139 nM | 219 nM | 161 nM |
| **CLK1** | **CLK2** | **FGFR2** | **PDGFRa** | **FLT3** |
| 512 nM | 112 nM | 320 nM | 956 nM | 714 nM |

**Figure 2.** Kinase selectivity profile of compound **24**.

At this point, we returned to the panel of 20 kinases used for optimization to obtain a more accurate picture of kinase selectivity for **24** (Fig. 2). Six kinases furnished an $IC_{50}$ less than 1 μM: the five that had shown greater than 80% inhibition in the selectivity count, and PDGFRa which had shown 71% inhibition. Additionally, compound **24** was more than 100-fold selective relative to RSK for the kinase panel, with the exception of LRRK2 and PRKD1, for which compound **24** showed 16- and 35-fold selectivity, respectively. We then expanded the kinase panel to include over 200 additional unique kinases. We were pleased to find that **24** had an $IC_{50}$ of less than 1 μM for only four other family members (PRKD2, PRKD3, RET, and FLT3). These results confirmed the power of the selectivity screening methodology developed for this program. By tracking a broader panel of potentially cross-reactive kinases at a single concentration, we were able to identify a compound with high selectivity vs. most of the readily testable portion of the kinome.

In summary, we followed up on the initial indole series leads **1**–**3** to further optimize potency, kinase selectivity and physical properties. Based on its overall balanced profile, compound **24**, BIX 02565, is an attractive candidate for use in vitro and in vivo to explore the role of RSK as a target for the treatment heart failure. Further results will be reported in due course.[10]

## Acknowledgements

The authors would like to express their gratitude to Dr. John Miglietta for determining the percent homology of the ATP pocket for the kinase selectivity panel versus the N-terminal ATP pocket of RSK2.

## References and notes

1. Karmazyn, M.; Sawyer, M.; Fliegel, L. *Curr. Drug Targets Cardiovasc. Haematol. Disord.* **2005**, *5*, 323.
2. Nakamura, T. Y.; Iwata, Y.; Arai, Y.; Komamura, K.; Wakabayashi *Circ. Res.* **2008**, *103*, 891.
3. (a) Karmazyn, M.; Kilic, A.; Javadov, S. *J. Mol. Cell Cardiol.* **2008**, *44*, 647; (b) Karmazyn, M.; Gan, X. T.; Humphreys, R. A.; Yoshida, H.; Kusumoto, K. *Circ. Res.* **1999**, *85*, 777.
4. (a) Moor, A. N.; Gan, X. T.; Karmazyn, M.; Fliegel, L. *J. Biol. Chem.* **2001**, *276*, 16113; (b) Maekawa, N.; Abe, J.-I.; Shishido, T.; Itoh, S.; Ding, B.; Sharma, V. K.; Sheu, S.-S.; Vlaxall, B. C.; Berk, B. C. *Circulation* **2006**, *113*, 2516; (c) Avkiran, M.; Cook, A. R.; Cuello, F. *Curr. Opin. Pharmacol.* **2008**, *8*, 133.
5. Boyer, S. J.; Burke, J.; Guo, X.; Kirrane, T. M.; Snow, R. J.; Zhang, Y.; Sarko, C.; Soleymanzadeh, L.; Swinamer, A.; Westbrook, J.; DiCapua, F.; Padyana, A.; Cogan, D.; Gao, A.; Xiong, Z.; Madwed, J. B.; Kashem, M.; Kugler, S.; O'Neill M. M. *Bioorg. Med. Chem. Lett.* **2011**. doi:10.1016/j.bmcl.2011.10.030.
6. Compounds were tested in the Kinase SelectScreen© Kinase Profiling service, www.invitrogen.com. Kinase inhibition data were determined using full length human proteins.
7. Vieth, M.; Higgs, R. E.; Robertson, D. H.; Shapiro, M.; Gragg, E. A.; Hemmerle, H. *Biochim. Biophys. Acta* **2004**, *1697*, 243.
8. Bouillot, AMJ; Daugan, AC-M; Dean, AW; Fillmore, MC. WO2008074824.

9. *Compound solubility was measured as follows*: In duplicate deep well plates, 6 μL of a 10 mM DMSO stock solution was spiked into pH 7.4 buffer, targeting 50–200 μM final concentrations. The final DMSO concentration was 0.5%. The samples were incubated for 16–18 h, filtered, and analyzed using a spectrophotometer. The UV spectra of samples and reference were scanned from 230 to 500 nm. Solubility is measured by comparing the ratio of the areas under the curves for reference and sample.
10. Shi, X.; Yan, C.; Brookes, P. S.; Berk, B. C. Manuscript in preparation.
11. Inhibition of the phosphorylation of the transcription factor CREB (cAMP Response Element Binding) by RSK2 in cells was determined according to the method described in: Boyer, S.; Gao, A.; Guo, X.; Kirrane, T.; Sarko, C.; Snow, R.; Soleymanzadeh, F.; Zhang, Y. WO2011071716.